Short Communication

The Performance of Li-doped LiCoO$_2$ for Li-ion Battery: A First-Principles Study

F. H. Ning[1], X. Gong[1], F. Y. Rao[1], X. M. Zeng[2], C. Y. Ouyang[1,]*

[1] Department of Physics, Jiangxi Normal University, Nanchang, 330022, P. R. China
[2] School of New Energy Science and Engineering, Xinyu University, Xinyu 338004, P. R. China
[*]E-mail: cyouyang@jxnu.edu.cn

Although numbers of fundamental and technical studies on metal-doped LiCoO$_2$ have been done in the past years, there still remains a gap of theoretical analysis on Li-substituted LiCoO$_2$, which can be called as Li-rich electrode. The atomic structure, electronic structure and average intercalation voltage of Li-doped LiCoO$_2$ are systematically studied in this paper by means of first-principles calculations. Results show that Li-doping and replacing Co in the LiCoO$_2$ compound can improve the comprehensive performance of the LiCoO$_2$ cathode, including the structural stability, the intercalation voltage, and the electrical conductivity.

1. INTRODUCTION

Rapidly development of new applications, such as electrical vehicles (EVs), has pushed researchers to find better electrodes within high energy density for lithium ion batteries (LIBs). LiCoO$_2$, a typical cathode material, is most widely used in the LIB industry [1]. The practical capacity of LiCoO$_2$ is about 130-150 mAh g^{-1} and the experimental charge/discharge potential plateau is around 4.0 V when it's half-delithiated [2-5].

In order to meet the increasing requirement of power tools, improving the energy density is a burning issue. The capacity and intercalation potential of the electrode material are usually among the energy density factors. Efforts have been made for many years to enhance these performances, such as doping, a common strategy. Various properties may be greatly enhanced by substituting some metals into LiCoO$_2$, such as transition metals like Cr [6], Mn [7], Fe [8], Ni [9-10], Rh [11] and non-transition metals like Mg and Al [12-15]. It somehow reduces the cost of Co. From the first principles

calculations, Al increases the potential as well as some other performances of $LiCoO_2$, but the conductivity become worse upon Al doping. In addition, Mg substitution can improve electrical conductivity without lattice change [14-15].

Though so many kinds of metal element were mentioned above, few researchers considered about the metal of Li as the substitutes, which can be called a rich lithium case. In this paper, we investigate the Li substitution system of $Li(Co_{1-x}Li_x)O_2$, and the atomic structure, electronic structure and the average voltage are systematically studied by means of first-principles calculations.

2. COMPUTATIONAL DETAILS

All the calculations are performed by the Vienna ab initio simulation package (VASP) [16] within density functional theory (DFT) and the projector augmented wave (PAW) method [17]. In our calculations, we use GGA + U method, in which a Hubbard U term is included to treat the Co-3d states. The value of U (the on-site coulomb term) is selected to be 4.91eV according to other reports [18], and our tests show that this value is suitable for the initial structure system and the doped structure system.

The initial structure of $LiCoO_2$ is modeled with a supercell of $12 \times LiCoO_2$ formula units. For the Li-doped $LiCoO_2$ system, a Co ion substituted by one Li ion rebuilding a $Li(Co_{11/12}Li_{1/12})O_2$ cell. All the calculations is processed with an energy convergence standard of 10^{-5} eV per formula unit and the final forces on all relaxed atoms are less than 0.005 $eVÅ^{-1}$. The Monkhorst-Pack [19] scheme with $3 \times 3 \times 1$ *k*-points mesh is used for the integration in the irreducible Brillouin zone. The cut-off energy for the plane waves is chosen to be 600 eV. Spin polarization has been taken into account, because the magnetic atoms play important roles in the electronic structure. The calculation of the density of states (DOS) is smeared by the Gaussian smearing method with a smearing width of 0.05 eV.

3. RESULTS AND DISCUSSION

3.1 The structure changes upon Li-doping

The $LiCoO_2$ is belonging to the α-$NaFeO_2$ type structure with a space group of $R\bar{3}m$. The $Li(Co_{11/12}Li_{1/12})O_2$ system is modeled by substituting the centre Co atom with a Li atom, and the system contains 13 Li atoms, 11 Co atoms and 24 O atoms. The proportion of substitution Li is about 8%. The 8% Mg-doped system has been calculated as a part of discussion on the difference between different doping elements by Xu's et al. [20]. In addition, Shi et al. have tried doping 8% Mg into $LiCoO_2$ by the first principles calculation, aiming at balancing effective and accuracy between calculations with experiments [4].
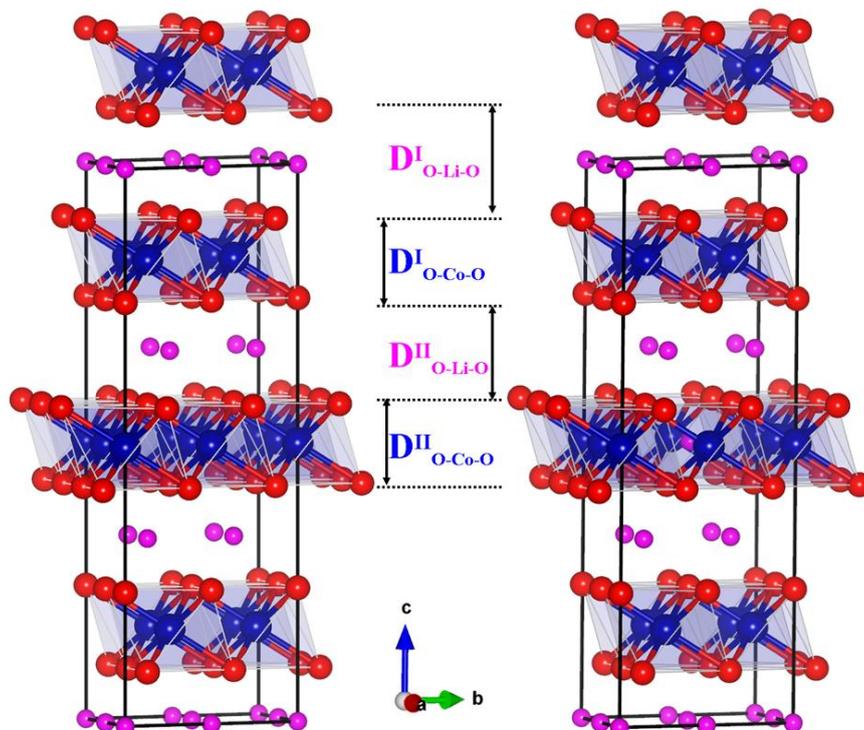
Figure 1. Schematic views of the atomic structures of $LiCoO_2$ (a) and $Li_{11/12}Co_{13/12}O_2$ (b). The middle (red), large (blue), and small (purple) spheres are O, Co and Li atoms, respectively. The symbols of "$D^{I/II}_{O-Li-O}$" and "$D^{I/II}_{O-Co-O}$" are the oxygen distance across the Li layer and across the cobalt atoms respectively.
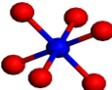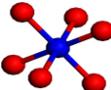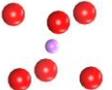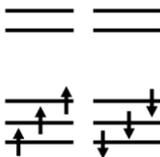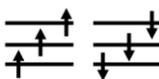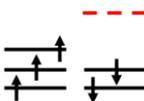
The relaxed structure of $LiCoO_2$ and $Li(Co_{11/12}Li_{1/12})O_2$ system is shown in Fig. 1, and the lattice constants is listed in Table 1, with the experimental reference [4] beside them. We can find that the lattice constants become larger after Li-doping, which is similar to the case of Mg doping in Xu's paper [20]. It would stand to reason that the undoped Co-O layer distance (D^I_{O-Co-O}) almost hasn't been change. Our calculated equilibrium oxygen distance across the Li layer ($D^{I/II}_{O-Li-O}$) or across the cobalt atoms ($D^{I/II}_{O-Co-O}$) indicates that the Li-doped Co-O layer distance expanding and the adjacent Li layer distance contracting after doping Li. It's due to the substitution Li^+ for Co^{3+}, which possesses less valence electron than the case of Co^{3+}.

Table 1. The relaxed structural parameters of $LiCoO_2$ and $Li(Co_{11/12}Li_{1/12})O_2$

System	a (Å)	b (Å)	c (Å)	c/a (Å)	Oxygen distance (Å)	
					$D^{I/II}_{O-Li-O}$	$D^{I/II}_{O-Co-O}$
$LiCoO_2$[4]	2.82	2.82	14.06	4.986	3.0940	2.8156
$LiCoO_2$	5.6642	5.6642	14.1647	\	2.652	2.070
$Li(Co_{\frac{11}{12}}Li_{\frac{1}{12}})O_2$	5.7077	5.7020	14.2082	\	2.655/2.632	2.071/2.112

Unlike Co^{3+}, the substitution Li^+ doesn't build strong coulomb interactions with the adjacent six oxygen atoms, and the distance between the doped lithium atom and oxygen atoms is longer than that of Co-O bond, as shown in Table 2. That's why the Li-doped Co-O slab distance expanding. The Co atoms adjacent to the substitution Li^+ make some responds to keep charge balance, two Co^{3+} change into Co^{4+}. From the structure information shown in Table 2, the Co-O bond lengths of Co^{4+} case are different from that of Co^{3+}, contains four shorter bonds and two normal bonds. Furthermore, the magnetic moment of Co^{4+} is 1.0 μ_B.

Table 2. Local structures and electronic configurations for different type of Co ion and the substitution Li ion

Type of Co ions	Co^{3+} in $LiCoO_2$	Co^{3+} in $Li(Co_{\frac{11}{12}}Li_{\frac{1}{12}})O_2$	Co^{4+} in $Li(Co_{\frac{11}{12}}Li_{\frac{1}{12}})O_2$	Li^+ in $Li(Co_{\frac{11}{12}}Li_{\frac{1}{12}})O_2$
Local structures around Co				
Magnetic moments (μ_B)	0	0	1	\
Co-O bond length or doped Li-O distance (Å)	1.935 1.935 1.935 1.935 1.935 1.935	1.948 1.947 1.964 1.964 1.943 1.943	1.878 1.877 1.894 1.894 1.945 1.944	2.031 2.031 2.019 2.017 2.031 2.031
	$(t_{2g}\uparrow)^3(t_{2g}\downarrow)^3$	$(t_{2g}\uparrow)^3(t_{2g}\downarrow)^3$	$(t_{2g}\uparrow)^3(t_{2g}\downarrow)^2$	\
Electronic configurations				\

3.2 Electronic structure

$LiCoO_2$ is identified to be p-type semiconductor. The conductivity of Li-doped system should be improved by the presence of Co^{4+}. The density of states (DOS) of $Li(Co_{11/12}Li_{1/12})O_2$ is shown in Fig. 2. It can be seen clearly that $Li(Co_{11/12}Li_{1/12})O_2$ remains semiconductive behavior and the band gap of Li-doped system becomes smaller, giving an evidence to the improved conductivity. Upon doping, the change of the electronic structure can be written as $3Co^{3+}\rightarrow 2Co^{4+} + Li^+$. The electronic structure variation is triggered by the two Co^{4+} and the six O in the Li-doped Co-O layer.
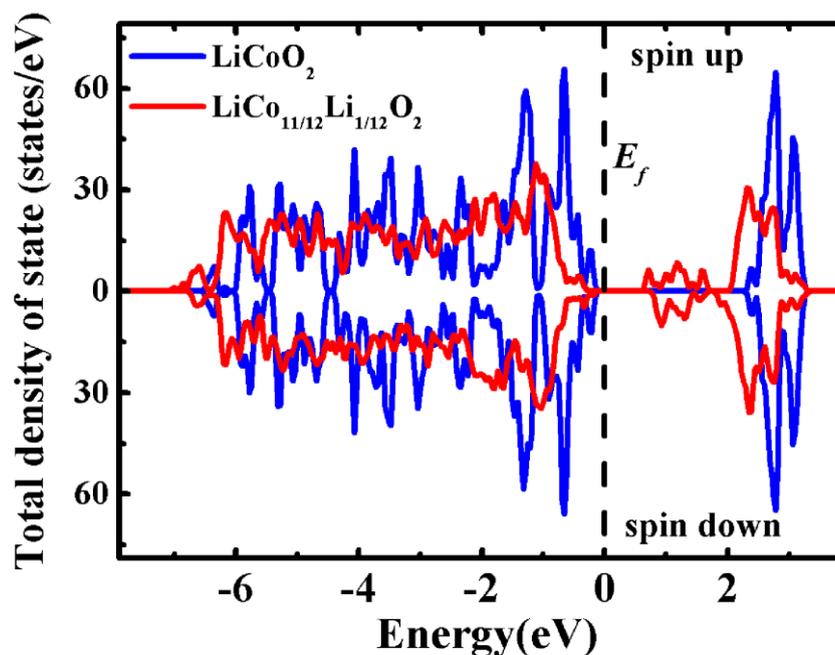
Figure 2. The total density of states of LiCoO$_2$ (blue) and Li(Co$_{11/12}$Li$_{1/12}$)O$_2$ (red).

In the case of LiCoO$_2$, cobalt keep in Co^{3+} state, which consistent with a 3d^6 electronic configuration, and the 3d-orbits split into t$_{2g}$ triplet and e$_g$ doublet in an octahedral crystal field.
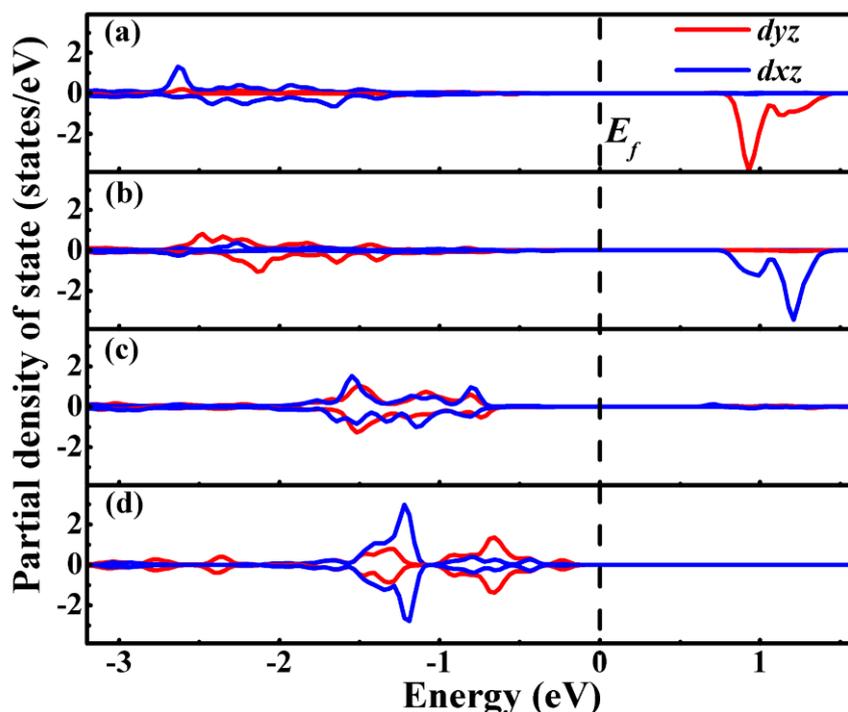

Figure 3. Partial density of dyz and dxz states of Co^{4+} in Li(Co$_{11/12}$Li$_{1/12}$)O$_2$ (a), (b); and Co^{3+} in Li(Co$_{11/12}$Li$_{1/12}$)O$_2$ and LiCoO$_2$ (c), (d).

As shown in Fig. 3(d), Co^{3+} exhibits low spin state with 3 electrons occupying the spin up t_{2g} orbits and the other 3 electrons occupying spin down t_{2g} orbits. The e_g orbits is unoccupied, thus leaving a band gap of about 2.4 eV. It's quite difficult for electronic transition at room temperature. However, in the case of $Li(Co_{11/12}Li_{1/12})O_2$, there are two Co^{4+} around the doped Li atom. Co^{4+} has loss one more electron than Co^{3+}, it means that the t_{2g} orbits remain an unoccupied orbit, as is shown in Fig. 3(a) and 3(b).

The partial density of Co-3d states is projected according to a coordinate system, which takes the Co atom for origin, the Co-O bonds for axis (marked in Fig. 4). The Co-3d projected density of states of (a), (b) and (c) in Fig. 3 stand for Co20, Co17 and Co14 in Fig. 4. The two Co^{4+} ions in $Li(Co_{11/12}Li_{1/12})O_2$ refer to Co20 and Co17, and the unoccupied t_{2g} orbits are d_{yz} and d_{xz}, respectively. The Co^{3+} ions in $Li(Co_{11/12}Li_{1/12})O_2$, taking Co14 for instance, are almost the same as the case of Co ions in $LiCoO_2$. In order to verify these, we plotted the induced charge density ($\Delta\rho$) in Fig. 4, which is defined as $\Delta\rho=\rho(Li(Co_{11/12})O_2)+\rho(3e^-)-\rho(Li(Co_{11/12}Li_{1/12})O_2)$. Where $\rho(Li(Co_{11/12})O_2)$ and $\rho(Li(Co_{11/12}Li_{1/12})O_2)$ are the charge density of the $Li(Co_{11/12}Li_{1/12})O_2$ system with and without Li in the Co-O slab. With this definition, positive isosurface values indicate that charge deficiency happened when it is compared with $LiCoO_2$ system. It's obvious that the charge deficiency of Co20 and Co17 are mainly distributed in the yz-plane and xz-plane respectively. It is in agreement with the results of density of Co-3d state in Fig. 3.
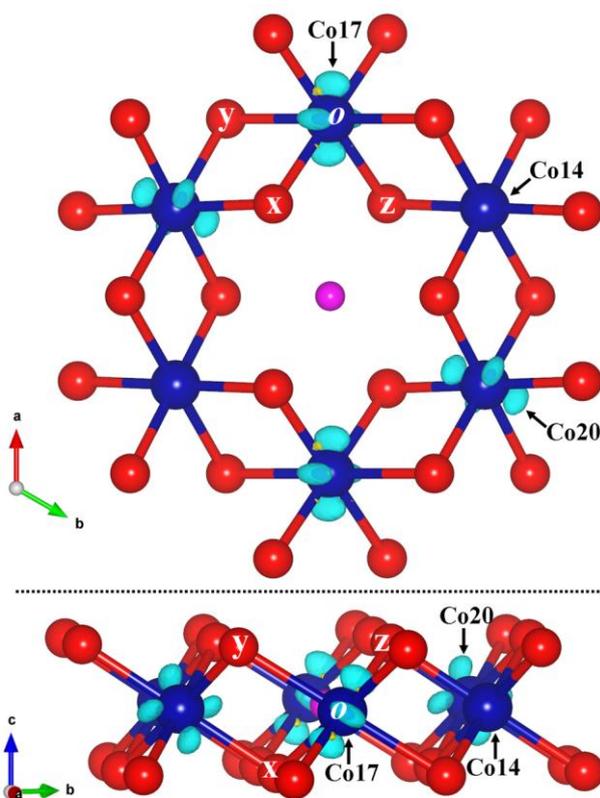

Figure 4. Charge density difference between $Li(Co_{11/12}Li_{1/12})O_2$ and $(Li(Co_{11/12})O_2 +3e^-)$. The red (middle), blue (large) and purple (small) spheres are O, Co and Li atoms, respectively. "x" ,"y", "z" and "o" refer to the orientation of the new coordinate system for projecting.

3.3 The average voltage and volume change upon delithiation

Then we calculated the average voltage of the $Li(Co_{11/12}Li_{1/12})O_2$ material. The average delithiation potential is defined as: [21-22]

$V_{ave} = -\Delta G/nF$

Where ΔG is the Gibbs free energy change after delithiation, F is the Faraday constant, and n is the Mole number of removed lithium ions. Assuming that the volume and entropy changes are negligible during the reaction, the average voltage can be approximately obtained from the internal energy. It's given by:

$V_{ave} = -\Delta E/nF$

Where ΔE is defined as:

$\Delta E = E[Li(Co_{11/12}Li_{1/12})O_2] - E[Li_x(Co_{11/12}Li_{1/12})O_2] - (1-x) E_{bcc}[Li]$

Where $E[Li(Co_{11/12}Li_{1/12})O_2]$ and $E[Li_x(Co_{11/12}Li_{1/12})O_2]$ are the total energy of $Li(Co_{11/12}Li_{1/12})O_2$ and $Li_x(Co_{11/12}Li_{1/12})O_2$ system, and $E_{bcc}[Li]$ is the total energy of metallic lithium in a body-centered-cubic (bcc) phase. And we have given the contrast analysis between $LiCoO_2$ and $Li(Co_{11/12}Li_{1/12})O_2$, as is shown in Fig. 5.

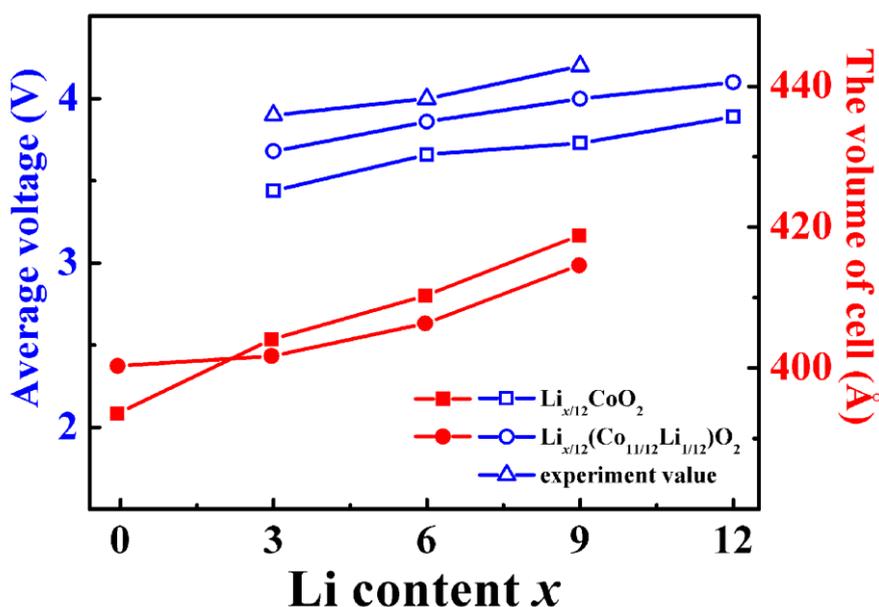**Figure 5.** The average delithiation voltage (blue line with open symbol) and the volume change (red line with solid symbol) of $LiCoO_2$ and $Li(Co_{11/12}Li_{1/12})O_2$ system.

The average intercalation potential of $Li(Co_{11/12}Li_{1/12})O_2$ is higher than that of $LiCoO_2$, which is similar to the Al-doped [12] or Mg-doped [23] case. The predicted average intercalation potential is around 3.86 V when half number of the Li is removed from $Li(Co_{11/12}Li_{1/12})O_2$, which is a little bit lower than the experimental charge/discharge potential plateau of about 4.0 V [2, 3]. The volume change is not as large as the $LiCoO_2$ system, which means that the structure is more stable after doping

with Li. This may be caused by the asymmetrical Co-O bonds induced by Co^{4+}, which enhanced the stability of CoO_6 octahedrons. In addition, there may be some relationship between the average intercalation potential and the volume changes.

4. SUMMARY AND CONCLUSIONS

In summary, when one out of 12 Co atoms in the Co-O layer is substituted by Li ($Li(Co_{11/12}Li_{1/12})O_2$), two Co^{3+} ions is turned into Co^{4+} ions with a distinctive local structure, which combined with four shorter and two longer Co-O bonds. It indicates that the electronic configuration of the Co-3d states become $(t_{2g}\uparrow)^3(t_{2g}\downarrow)^2$ with a magnetic moment of 1.0 μB, which is different to that of $(t_{2g}\uparrow)^3(t_{2g}\downarrow)^3$ in non-magnetic Co^{3+} ions in the pure $LiCoO_2$. As a result, the electrical conductivity can be improved upon doping. The cell volume expanded with the Li-doped Co-O layer distance expanded and the adjacent Li layer distance contracted. The structural stability can also be enhanced as the volume expansion is suppressed upon Li-doping. The average voltage is increased, which is beneficial to enhance the energy density of the battery system. Given these advantages, it is expected that Li-doping is a good strategy to enhance the performance of $LiCoO_2$ as cathode material for in lithium-ion battery.

References

1. J. B. Goodenough, K. Youngsik, *Chem. Mater.*, 22 (2010) 587.
2. Z. X. Wang, L. J. Liu, L. Q. Chen, X. J. Huang, *Solid State Ionics*, 148 (2002) 335.
3. L. J. Liu, L. Q. Chen, X. J. Huang, X. Q. Yang, W. S. Yoon, H. S. Lee and J. McBreenb, *J. Electrochem. Soc.*, 151 (2004) A1344.
4. S. Q. Shi, C. Y. Ouyang, M. S. Lei and W. H. Tang, *J. Power Source*, 171 (2007) 908-912.
5. F. Xiong, H. J. Yan, Y. Chen, B. Xu, J. X. Le and C. Y. Ouyang, *Int. J. Electrochem. Sci.*, 7 (2012) 9390-9400.
6. C. D. W. Jones, E. Rossen, J. R. Dahn, *Solid State Ionics*, 68 (1994) 65.
7. R. Stoyanova, E. Zhecheva, L. Zarkova, *Solid State Ionics*, 73 (1994) 233.
8. H. Kobayashi, H. Shigemura, M. Tabuchi, H. Sakaebe, K. Ado, H. Kageyama, A. Hirano, R. Kanno, M. Wakita, S. Morimoto and S. Nasu, *J. Electrochem. Soc.*, 147(3) (2000) 960-969.
9. M. Y. Song, H. Rim, H. R. Park, *Ceram. Int.*, 39(5) (2013) 6937-6943.
10. K. K. Lee, K. B. Kim, *J. Electrochem. Soc.*, 147(5) (2000) 1709.
11. S. Madhavi, G. V. Subba Rao, B. V. R. Chowdari and S. F. Y. Li, *J. Electrochem. Soc.*, 148(11) (2001) A1279-A1286.
12. G. Ceder, Y. M. Chiang, D. R. Sadoway, M. K. Aydinol, Y. I. Jang and B. Huang, *Nature*, 392 (1998) 694.

13. A. A. Popovich, M. Yu. Maximov, A. M. Rumyantsev and P. A. Novikov, *Russ. J. Appl. Chem.* 88(5) (2015) 898-899.
14. H. Tukamoto, A. R. West, *J. Electrochem. Soc.*, 144(9) (1997) 3164-3168.
15. J. H. Cheng, C. J. Pan, C. Nithya, R. Thirunakaran, S. Gopukumar, C. H. Chen, J. F. Lee, J. M. Chen, A. Sivashanmugam and B. J. Hwang, *J. Power Source* 252 (2014) 292-297.
16. G. Kresse, J. Furthmuller, *Phys. Rev*. B, 54 (1996) 11169.
17. G. Krosse, J. Joubert, *Phys. Rev.* B, 59 (1999) 1758.
18. F. Zhou, M. Cococcioni, C.A. Marianetti, D. Morgan, G. Ceder, Phys. Rev. B, 70 (2004) 235121.
19. H. J. Monkhorst, J. D. Pack, *Phys. Rev.* B, 13 (1976) 5188.
20. X. G. Xu, C. Li, J. X. Li, U. Kolb, F. Wu and G. Chen, *J. Phys. Chem*. B, 107 (2003) 11648-11651.
21. C. Wolverton and Alex Zunger, *Phys. Rev. Lett*., 81(3) (1998) 606.
22. M. K. Aydinol, A. F. Kohn, G. Ceder, K. Cho and J. Joannopoulos, *Phys. Rev. B*, 56 (1997) 1354.
23. Z. G. Wang, Z. X. Wang, H. J. Guo, W. J. Peng and X. H. Li, *Ceram. Int.*, 41(1) (2015) 469-474.